Int J Clin Exp Med 2019;12(7):8032-8043
www.ijcem.com /ISSN:1940-5901/IJCEM0090449

Original Article

Histone acetyltransferase TIP60 mediates spermatozoa damage induced by microwave irradiation in rats

Xuan Wei[1], Wei Yan[1], Guo-Ping Wang[2], Long-Fang Zhang[1], Ying Jin[1], Ti-Ye Sun[1,3]

[1]Department of Gerontology, General Hospital of The Air Force, Haidian, Beijing 100142, P. R. China; [2]Center for Disease Control of Zhifu District, Yantai City 264000, Shandong Province, P. R. China; [3]Department of Oncology, Hospital of He Bei Yanda, Sanhe 065201, Hebei Province, P. R. China

Received December 26, 2018; Accepted April 9, 2019; Epub July 15, 2019; Published July 30, 2019

Abstract: The aim of the current study was to investigate the effects of microwave irradiation on rat spermatozoa, examining the roles of histone acetyltransferase TIP60 in this process. Laboratory rats (n=54) were randomly divided into the control group, radiation group, and radiation + Traditional Chinese Medicine (TCM) group. Rats in the radiation and TCM groups received radiation for 15 minutes at 100 mW/cm^2. The TCM group was treated with intragastric administration once a day for 7 days after radiation. On days 1, 2, 7, and 14 after radiation, rat semen/testis was collected. Sperm motility was measured. Hematoxylin and eosin staining was performed on testis sections. Terminal deoxynucleotidyl transferase dUTP nick-end labelling was used to detect apoptosis of spermatogenic cells. The ultrastructure of the sperm was observed by electron microscopy. TIP60, p53, and tubulin expression was detected by Western blot analysis. Testis sections of the rats demonstrated dyszoospermia in the radiation group, compared with controls, but lighter than the TCM group. Ultrastructure imaging of sperm in the radiation group demonstrated oligospermatism, dolichocephalia, trochocephalia, congenital acrosome absence, and mitochondrial disorder. There was a regular cell layer, high sperm density, and sharp axoneme in the TCM group. Following radiation, the percentage of apoptotic androgones was remarkably increased. At day 1 and day 2, the percentage was significantly higher in the radiation group than in the TCM group ($P<0.05$). At days 7 and 14, it was decreased, compared with earlier time points, but remained significantly higher than the TCM group (18.51±3.58) and control group ($P<0.05$). At days 1, 2, and 14, sperm counts in the TCM group (24.67±3.55, 21.40±2.21 and 25.60±4.68) were significantly different from the radiation group (34.50±3.43, 8.83±0.19 and 13.50±2.35; $P<0.05$). At day 7, counts were significantly lower in the radiation group than the control group ($P<0.05$). Sperm density levels and percentages of grade A + B sperm were also measured. They were ameliorated by TCM treatment following radiation. TIP60 expression was detected in semen by Western blotting on day 1, day 2, and day 14. At days 1, 2, and 14, p53 expression was higher in the TCM group than the radiation group. The mechanism of sperm injury by radiation may be that radiation damages DNA. This damage increases TIP60 histone acetyltransferase activity and promotes p53 acetylation. As a downstream target of TIP60, p53 can regulate repair of damaged DNA. In conclusion, TCM treatment increases p53 expression and reduces sperm radiation damage.

Keywords: TIP60, acetylation, microwave irradiation, sperm

Introduction

More and more people work with communication instruments. Thus, microwave irradiation has become a concern. It may have an impact on human health. The effects of electromagnetic radiation on reproductive health in males has drawn much attention. In a previous preliminary study [1], microwave irradiation was demonstrated to damage sperm morphology, ultra-structural organization, apoptosis, and movement.

Histone acetyltransferase (HAT) TIP60 was initially identified as a protein that binds to the Tat protein in HIV [2], as the most common HAT in the MYST family members. TIP60 could catalyse the transfer of an acetyl group to the ε-amino of lysine in H4 and H2A histones. Recombinant TIP60 protein can acetylate the lysine 14 of H3 *in vitro*. Upon DNA damage, TIP60 acetylates lysine 20 of p53. This is critical in regulating p53-dependent cell apoptosis and repairing of double stranded breaks (DSBs) [3, 4]. Therefore, TIP60 activity is important in

sustaining genomic integrity and regulating repair of DNA damage [5, 6].

Ingredients of TCM extracts used in the present study included herba cistanches, Morinda officinalis, Herba Epidmed II, Angelica sinensis, roots of red-rooted salvia, Radix Polygoni Multiflori Preparata, Solomon's seal, seeds of Chinese dodder, fructus ligustri lucidi, the fruit of Chinese wolfberry, radix pseudostellariae, Born astragalus, fructus cnidii, and Shudi. They have been previously demonstrated to protect against the damaging effects of radiation [1]. Therefore, an *in vivo* study was performed to investigate the mechanisms of TIP60 regulation of rat spermatozoa damage caused by microwave irradiation.

Materials and methods

Animals and groups

Adult male Wistar rats (n=54; weight, 250±20 g) were obtained from and fed in the Laboratory Animal Center of Academy of Military Medical Sciences, Beijing, China. They were divided into 3 groups randomly, including the control group (n=6), radiation group (n=24), and drug treatment group (n=24). All mice were fed with a standard diet and maintained in a temperature-controlled room (22-25°C, 45% humidity) with a 12-hour dark-light cycle. The current study was approved by the Ethics Committee of the Academy of Military Medical Sciences, Beijing, China.

Instruments and materials

Laser scanning microscope (LSM510; Carl Zeiss AG, Oberkochen, Germany); AMT Camera System and Transmission Electron Microscope (TEM; Philips Medical Systems, Inc., Bothell, WA, USA); Rabbit anti-TIP60 antibody (cat. no. SAB4500117, Sigma-Aldricht; Merck KGaA); Specific and non-specific acetylation antibodies were obtained from Professor Yao (University of Science and Technology of China, Beijing, China); Terminal deoxynucleotidyl transferase dUTP nick-end labelling (TUNEL) apoptosis kit (Wuhan Boster Biological Technology, Ltd., Wuhan, China).

Traditional Chinese medicine (TCM) preparation

TCM used in the current study was obtained from Beijing Tongrentang Drug Store (Beijing, China). Constituents of the TCM medicine included *Cistanche deserticola*, *Morinda officinalis*, *Epimedium*, *Angelica*, *Salvia miltiorrhiza* Radix polygoni multiflori preparata, *Polygonatum sibiricum*, dodder, Glossy privet fruit, *Lycium barbarum*, Radix pseudostellariae, Astragalus root, Fructus cnidii, Radix rehmanniae, and radix praeparata, as well as others. Each component was administered with dosage of 140 g. The crude TCM was decocted with water to a final concentration of 1 g/mL for use in the study. The prepared drug was stored at 4°C in sealed flasks.

Dose calculation

In the current study, rats were treated with 5 times the dosage of that in the human body (65 kg) by intragastric administration. Dosage (rat) X/weight (rat)=5 × Dosage (human)/65 kg.

Microwave irradiation and treatment

In the radiation group, 12 rats were placed in an anechoic chamber without a reflection coefficient. They received whole-body uniform irradiation once with 100 mW/cm^2 density for 15 minutes at 18±2°C and 50-70% humidity. Following irradiation, 6 rats in each cage were fed as usual with free food and water. The remaining 12 rats were received the same irradiation process in the anechoic chamber at 18°C. In the treatment group, 12 rats were placed in the anechoic chamber without a reflection coefficient. They received whole-body uniform irradiation once with 100 mW/cm^2 of density for 15 minutes at 18±2°C and 50-70% humidity. Following irradiation, 6 rats in each cage were fed as usual. On day 1 after irradiation, the rats were treated with drugs at doses according to their weight, calculated as Dosage (rat) X/weight (rat)=5 × Dosage (human)/65 kg, by intragastric administration once a day for 7 days. In the controls group, the rats were maintained in the chamber at 18±2°C without irradiation and fed normally.

Sample collection

According to previous methods [7], on days 1, 2, 7, and 14 after irradiation, serum, testicles, epididymis, and sperm were collected from the 6 rats in the radiation and treatment groups, as well as from 3 rats in the control group at days 7 and 14 after radiation.

Blood samples were collected from the femoral artery into anti-coagulative tubes. Samples were centrifuged at 3,000 × g for 10 minutes to separate serum, then stored at 4°C. Testicles and the epididymis were separated from adipose tissue and weighed, calculating organ coefficients. Left testicles and the epididymis were fixed in 10% formalin. The right epididymis was cut into two uniform halves along the vertical axis. It was then cut into six uniform sections along the lateral axis. The sections were placed in 1 mL incubating buffer [0.5% bovine serum albumin (BSA; Beijing Baiaolaibo technology Co., LTD) diluted in PBS] at 25°C. The sections were washed with incubating buffer and transferred to the washing buffer (8 g NaCl, 0.2 g KCl, 0.24 g KH_2PO_4, 3.628 g Na_2HPO_4. $12H_2O$ diluted in 1 L H_2O, PH 7.4) in tubes.

The vas deferens was separated from the epididymis tail and prostate. Incubating buffer (1 mL) was then injected into the broken end of the vas deferens to wash it. The aim was to collect all sperm cells. They were then incubated at 37°C for 30 minutes.

Analysis of rat semen

Semen quality was analyzed using a semen analyzer (WLJY-9000; Weili New Century Science & Tech. Deve Co. Ltd., Beijing, China), combined with a platform, temperature controller, and MACRO count board. Sperm motility, grade A sperm motility (%), grade B sperm motility (%), grade C sperm motility (%), and grade D sperm motility (%) were recorded according to the World Health Organization laboratory manual for examination and processing of human semen [7].

Pathological examination of on rat testes and epididymis

Testes and epididymis tissue sections (2 mm) were embedded in wax and stained with hematoxylin and eosin at room temperature. Pathological changes in interstitial cells and vessels were observed under the AMT Camera System transmission electron microscope (Phillips Healthcare, Amsterdam, The Netherlands), including spermatogenetic cell morphology and structure in seminiferous tubules. The spermatic cord and fascia tissue in the left testicles and epididymis were resected and washed with saline. They were fixed in 10% formalin and washed with water for 10-20 minutes. After dehydration, permeabilization was conducted using Aurion R-Gent SE-EM Kit (Head Beijing Biotechnology Co., LTD; www.hedebio.com/). Next, waxing and embedding was conducted. Tissues were then cut into sections and dried, dewaxed, stained, dehydrated, and sealed for imaging.

Apoptosis detection by TUNEL assay

Testicle samples were fixed in 10% formalin for 24 hours. They were then embedded in wax and cut into 4 μm serial sections. One section in each sample was analyzed by TUNEL to determine the apoptosis index (AI).

The samples were incubated in 0.5% Triton X-100 at 37°C for 1 hour and washed with 0.3% BSA in PBS. They were and incubated with the buffer containing terminal DNA transferase (TDT) and biotin-labelled dNTPs at 37°C for 1 hour. Sections were washed and incubated with streptavidin-fluorescein isothiocyanate at 37°C for 20 minutes. They were then stained with propidium iodide (50 μg/mL) for 15 minutes. Nuclei with yellow and brown staining indicated apoptotic cells. PBS was used as a negative control instead of TDT.

AI calculation: 5 fields (× 400) in each section were captured and the percentage of apoptotic cells in a total of 500 cells was calculated.

Sperm ultrastructure observation

Semen samples were centrifuged at 2,000 × g for 10 minutes at 4°C. The supernatant was discarded and added into 2.5% glutaraldehyde for 15 minutes. They were washed with PBS buffer for 2-3 hours at room temperature, then centrifuged at 2,000 × g for 10 minutes at 4°C. The supernatant was discarded and fixed in osmic acid for 0.5-1 hours. Following washing, the semen was dehydrated, embedded in epoxy resin, cut into semi-thin sections, and stained with toluidine blue. Following conformation by light microscope, the ultrathin sections were cut and observed with an AMT camera system (Advanced Microscopy Techniques, Corp., Woburn, MA, USA).

TIP60, p53, and tubulin expression in sperm

Semen was centrifuged at 2,000 × g for 10 minutes. The supernatant was discarded and 0.5 mL of sample buffer (7 ml 0.5 M Tris (pH

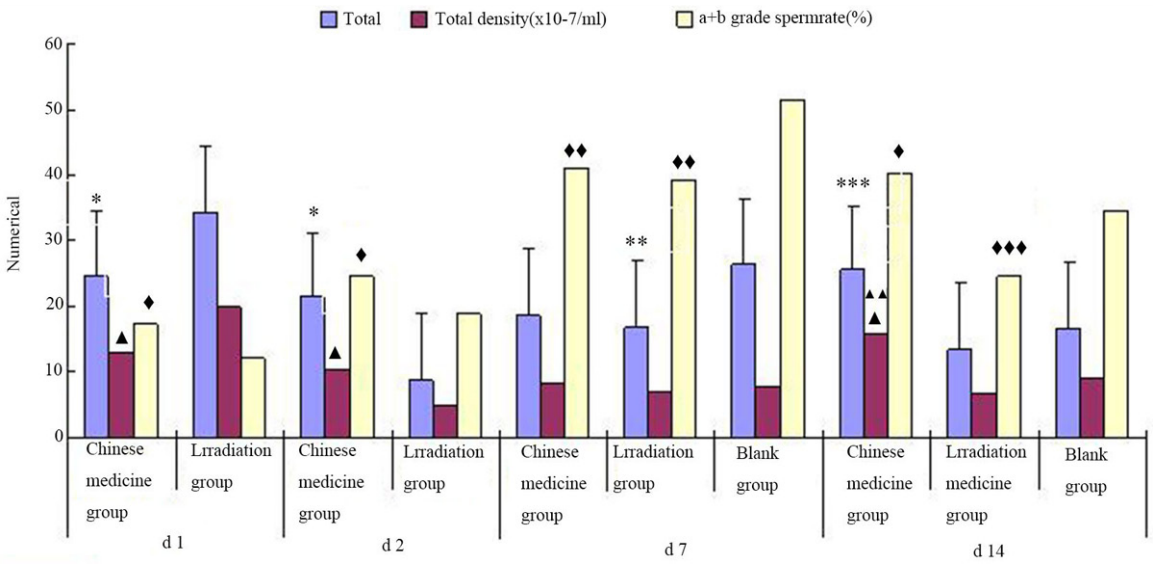

Figure 1. Routine analysis of sperm from rats in control, radiation, and treatment groups. Total sperm count, sperm density, and grade A + B motility rates were measured in each group.

7.8), 2.6 ml Glycerol, 1 μL DTT, 60 uL of 10% Brom Blue, 400 uL 10% SDS) was added. The samples were incubated at 100°C for 15-20 minutes and stored at -80°C.

Samples were separated on a 10% gel with 40-70 μl protein (2.5 ug/ul) quantification using the bicinchoninic acid method. Proteins were then transferred to a PVDF membrane with 120 V constant voltage for 90 minutes. The membrane was stained with ponceaus and blocked with 1% non-fat milk in TBS Tween at room temperature for 1-2 hours (TBST). Rabbit anti-tubulin (DM1A; 1:5,000, Shanghai Huayi Biotechnology Co., Ltd.), mouse anti-p53 (DO-1; 1:2,000, Shanghai Haoran Biotechnology Co., Ltd), and mouse anti-TIP60 (1:1,000, Shanghai Ruiqi Biotechnology Co., Ltd) antibodies diluted in 0.05% Tween in TBS were incubated with the blot at 4°C overnight. The blots were washed with TBST four times, 5-10 minutes each time. Secondary antibodies labelled with horseradish peroxidase (1:5,000, Beijing Solarbio Science & Technology Co., Ltd., Beijing, China CAS: SE131) were used for incubation at 25°C for 45 minutes. Blots were then washed with TBST four times, 5-10 minutes each time. An enhanced chemiluminescence system (Shanghai kemin Biotechnology Co., Ltd.) was used for signal detection.

Statistical analysis

Data were analyzed using SPSS 18.0 software (SPSS, Inc., Chicago, IL, USA). Data are presented as the mean ± standard deviation and were analyzed using one-way analysis of variance, followed by Tukey's test. $P<0.05$ indicates statistically significant differences.

Results

Routine analysis of rat semen

As presented in **Figure 1**, there were more sperm in the TCM group than the radiation group. At 1, 2, and 14 days, sperm counts in the TCM group (24.67±3.55, 21.40±2.21 and 25.60±4.68, respectively) were significantly different from that in the radiation group (34.50±3.43, 8.83±0.19 and 13.50±2.35, respectively; $P<0.05$). At 7 days, the sperm count in the radiation group (16.80±4.32) was significantly lower than the control group (26.50±3.23; $P<0.05$). At 14 days, it was higher in the TCM treatment group (25.60±4.68) than the control group (16.67±3.38; $P<0.05$).

At 1, 2, and 14 days, sperm density in the TCM-treated group (12.88±2.45, 10.38±0.18 and 15.70±1.32, respectively) was significantly different from that in the radiation group

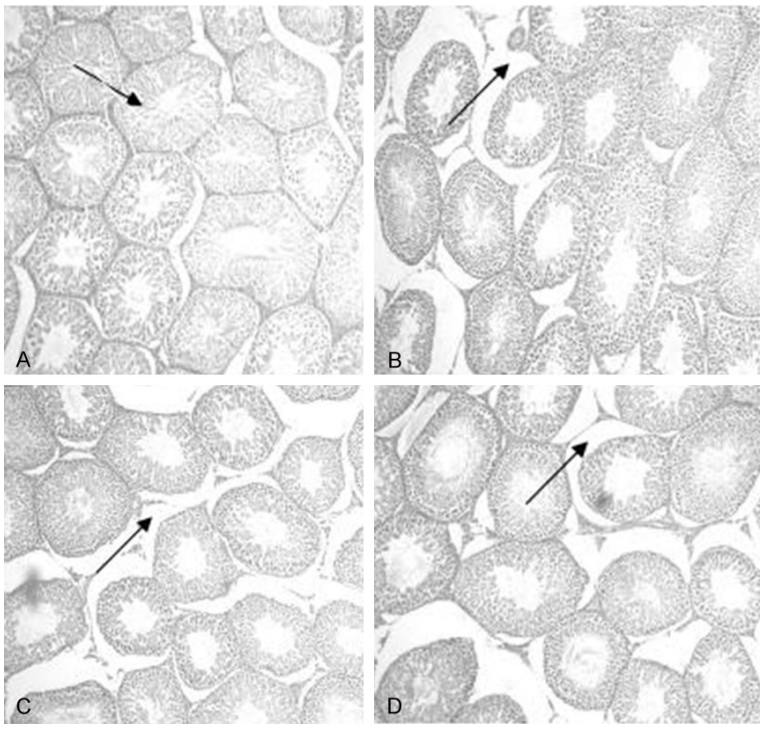

Figure 2. Testes sections from radiation group rats. (A) Day 1 (left); (B) Day 2 (left); (C) Day 7 (right); (D) Day 14 (left). LSM510 Laser scanning Confocal Microscopy (magnification, × 10,000-15,000).

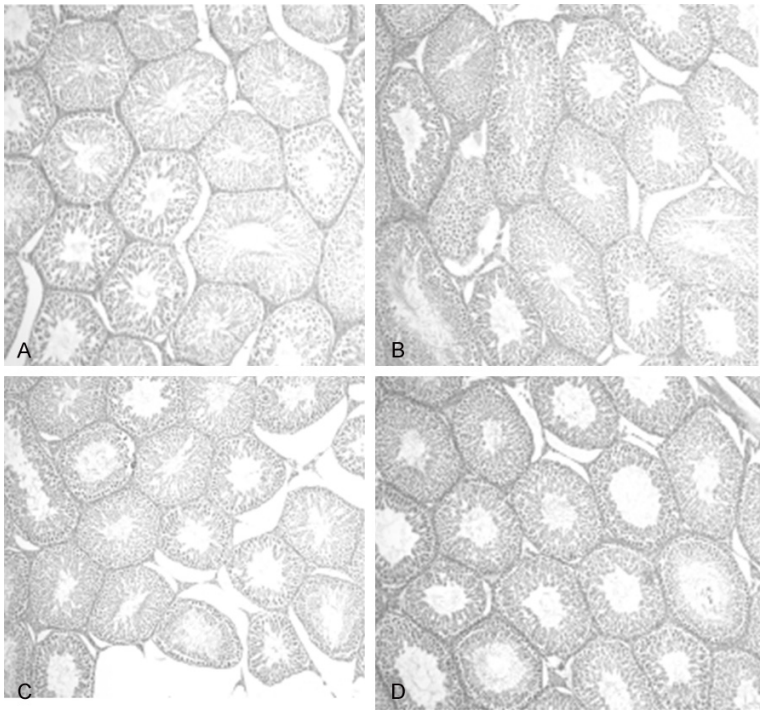

Figure 3. Testes sections from Traditional Chinese Medicine treatment group rats. (A) Day 1 (right); (B) Day 2 (right); (C) Day 7 (left); (D) Day 14 (right).

(19.88±2.57, 4.95±0.36 and 6.60±1.01, respectively; P< 0.05). At 14 days, sperm density in the TCM-treated group (15.70±1.32) was significantly higher than that in the control group (9.01±0.52; P<0.05).

At 1, 2, and 14 days, the percentage of grade A + B sperm in the TCM-treated group (17.36±2.87, 24.48±3.20 and 40.42±1.54, respectively) was significantly higher than that in the radiation group (12.28± 2.69, 18.96±3.79 and 24.50± 2.75, respectively; P<0.05). At 7 days, the percentage of grade A + B sperm in the control group (51.57±1.46) was significantly higher than that in the TCM-treated group (41.21± 3.87) and radiation group (39.41±4.08; P<0.05). At 14 days, the percentage of grade A + B sperm in the radiation group (24.50±2.75) was significantly lower than that in the control group (34.64±0.56; P<0.05). Current results demonstrate that the sperm number in the TCM-treated group was more than that in the radiation group. After 1, 2 and 14 days, the sperm number did not change much in the TCM-treated group. However, it was obviously altered in the radiation group. At 7 days, the sperm number was less in the radiation group than the TCM-treated group and control group. At 14 days, the sperm number in the TCM-treated group was higher than that in the radiation group and control group.

At 1, 2, and 14 days, sperm density in the TCM-treated group first increased, then decreased. Sperm density decreased all the time in the

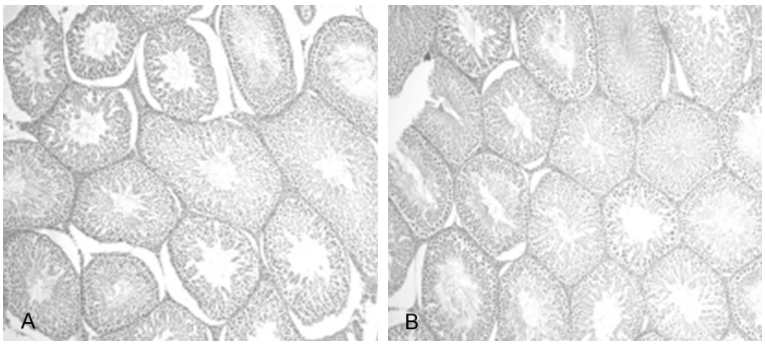

Figure 4. Testes sections from control group rats. (A) Day 7 (left); (B) Day 14 (right).

radiation group, compared with control group. At 14 days, it was higher in the TCM-treated group than in the radiation group and control group.

After 1, 2, and 14 days, the percentage of grade A + B sperm increased gradually in the TCM-treated group, while it slowly increased in the radiation group at 7 das, compared with the control group (51.57±1.46). The percentage of grade A + B sperm was decreased in TCM-treated (41.21±3.87) and radiation group (39.41±4.08). Differences showed statistical significance ($P<0.05$). At 14 days, compared with the control group (34.64±0.56), the radiation group (24.50±2.75) dramatically decreased, $P<0.01$.

Pathological examination of testes and epididymis

In the radiation group, the number of unregular seminiferous tubules increased. Limiting membrane thinning was observed. Seminiferous epithelium thinning and spermatogenic cells were not seen anymore. Sperm on the luminal surface decreased, as well as in interstitial cells in testis. There was hyalinization of interstitial tissues of testis and degeneration of part of the sertoli cells in seminiferous tubules (**Figure 2**).

Results of the TCM-treated group demonstrated that the seminiferous tubules were normal, with abundant mesenchyme containing capillaries. They were without obvious changes of the limiting membrane and tubular epithelium, with more spermatogenic cells and sperm on the luminal surface. There was less disorder of spermatogenic cells, immature spermatogenic cells falling in seminiferous tubule lumen, androgones falling off in seminiferous tubules, and sparse interstitial cells in testis (**Figure 3**).

In the control group, the seminiferous tubules displayed fullness, with a uniform and complete limiting membrane. There was moderate thickness of the seminiferous epithelium, spermatogenic cells, and mature sperm in different development stages, and sperm with moderate density in the lumen. Interstitial cells were arranged regularly in the testis and abundant in micro vessels in loose connective tissue (**Figure 4**).

Androgone apoptosis

Following irradiation, the percentage of apoptotic androgones increased, compared with control and TCM-treated group (**Figure 5**). At 1 and 2 days, the percentage of apoptotic androgones was 39.54±5.34 and 40.39±4.20, respectively, in the radiation group, significantly higher than that in the TCM-treated group (20.76±3.46 and 25.47±2.76, respectively; $P<0.05$). At 7 days, the percentage of apoptotic androgones decreased, compared with 1 and 2 days, but it was higher in the radiation group (30.66±5.22) than the TCM-treated group (18.51±3.58) and control group (15.66±4.35; $P<0.05$). At 14 days, the percentage of apoptotic androgones was significantly higher in the radiation group (23.50±2.35) than the TCM-treated group (10.84±3.28) and control group (12.56±2.82; $P<0.05$). There were no significant differences between the TCM-treated group and control group. Results are demonstrated in **Figure 5**.

Sperm ultra-structure observation

TEM results revealed that the sperm membrane was complete with regular mitochondria in the control group. Sperm in the radiation group exhibited oligospermatism, dolichocephalia, trochocephalia, congenital acrosome absence, and mitochondria disorder, while the TCM-treated group demonstrated a regular cell layer, high sperm density, and sharp axoneme (**Figure 6**).

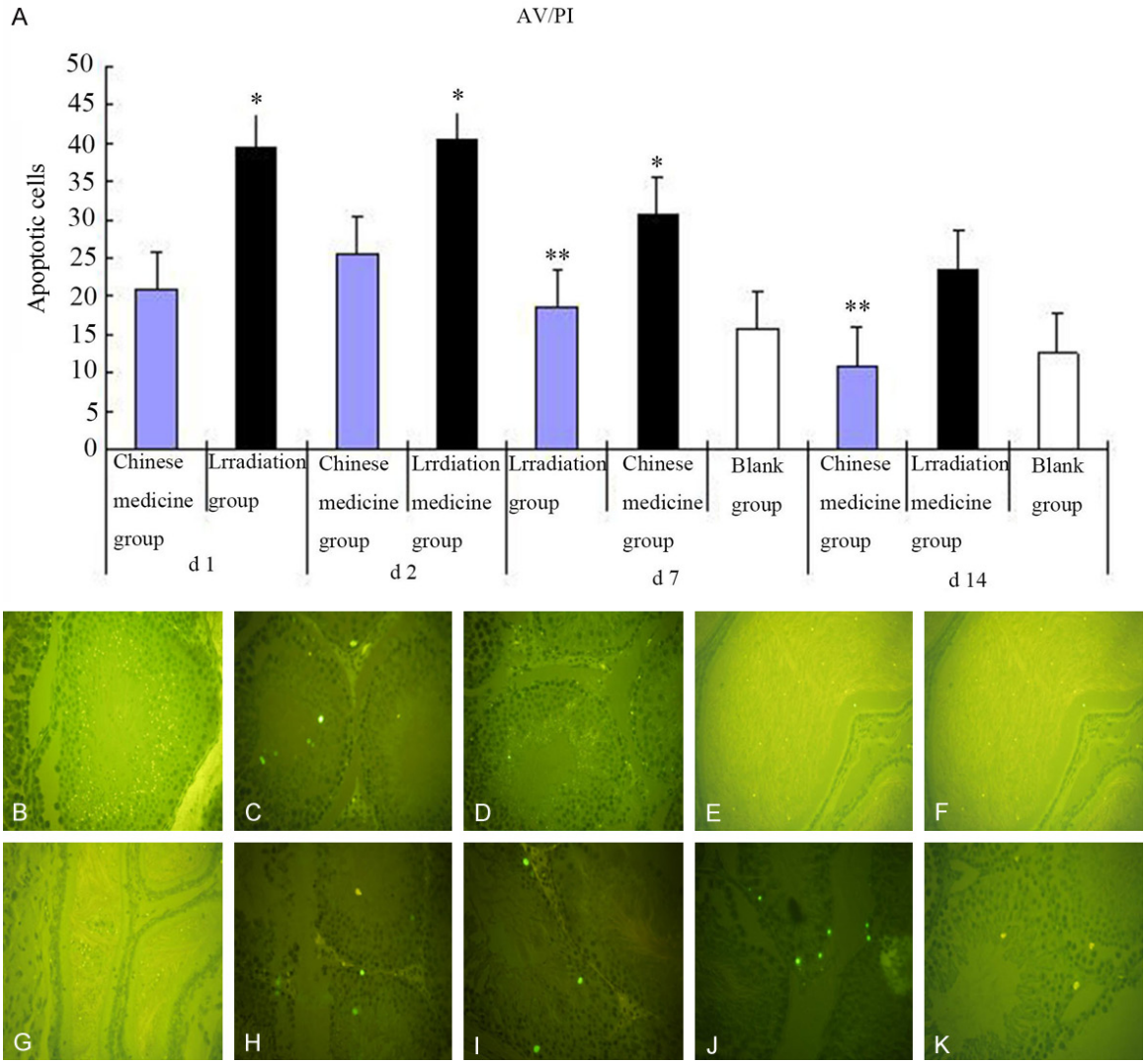

Figure 5. Under Eclipse TS100 inverted microscope: (A) Apoptosis of androgones in the control, radiation, and Chinese medicine treatment groups at different time points. TUNEL staining was performed on samples from (B) Radiation group at day 1 (left), (C) Treatment group at day 1 (right), (D) Radiation group at day 2 (left), (E) Treatment group at day 2 (right), (F) Control group at day 7 (left), (G) Radiation group at day 7 (right), (H) Treatment group at day 7 (left), (I) Control group at day 14 (right) and (J) Radiation group at day 14 (left), (K) Treatment group at day 14 (right).

TIP60 and p53

TIP60 expression was detected at 1 day (**Figure 7**) but was not detected at 2 days (**Figure 8**) and 14 days (**Figure 9**). At 1, 2, and 14 days, expression of p53 was higher in the TCM-treated group than the radiation group. There was no deviation in tubulin expression between the groups.

Discussion

In a previous study, Wang et al. (8) used a high-power wavelet (HPM; 0, 3, 10, 30 and 100 mW/cm^2) to treat 165 male Wistar rats for 5 minutes. After 6 hours and 1, 3, 7, 14, 28, and 90 days, testicle histomorphology was observed under a light and electron microscope. Results indicated that 3-100 mW/cm2 HPW, could damage androgones and induce pathological changes, including cell degeneration, necrosis, multinucleated giant cells forming, oligospermatism, and interstitial edema. TCM could protect cells from radiation damage, showing effects on TIP60. Androgone damage included death and had localized, ununiformed, and periodic characteristics. As the HPW increased, degeneration was aggravated. After 1 day of 3

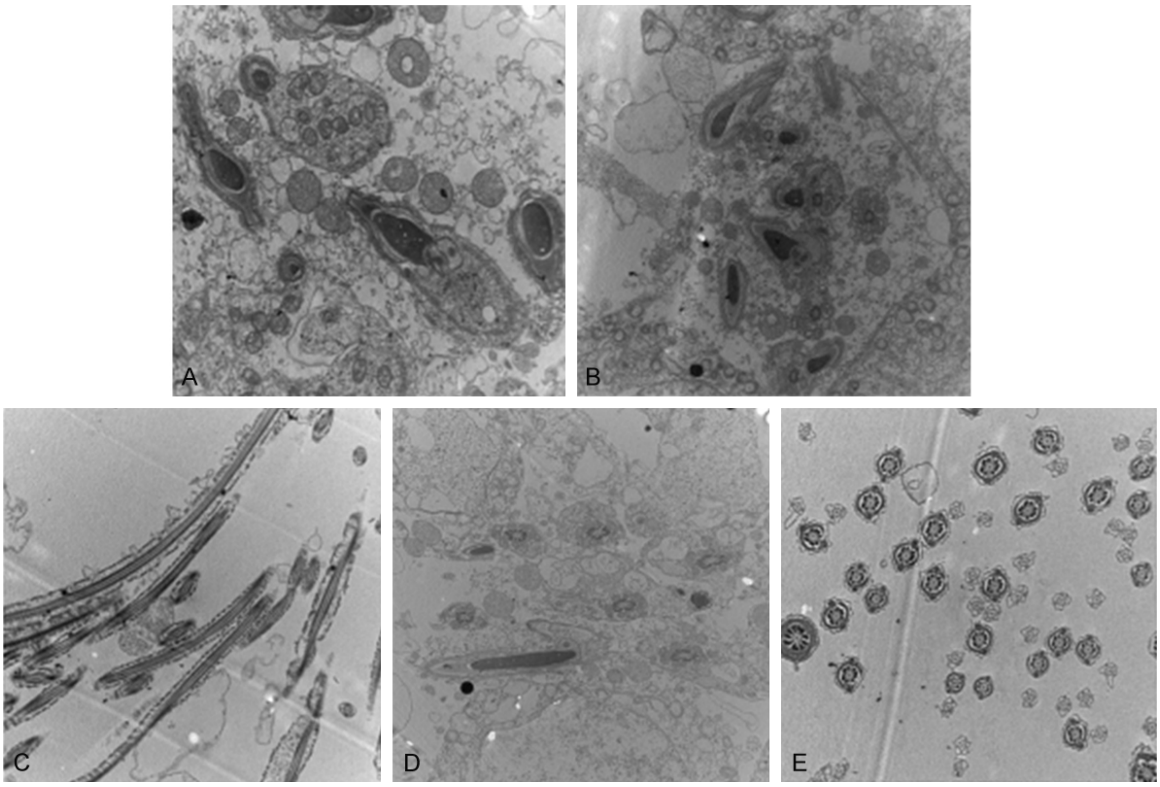

Figure 6. Transmission election microscopy imaging of semen samples. (A) Semen from the radiation group, exhibiting oligospermatism, dolichocephalia, trochocephalia, congenital acrosome absence, and mitochondria disorder (× 12,000); and (B) Semen in the TCM treatment group, exhibiting regular cell layer, large sperm density, and sharp axoneme (× 8,000); (C) Longitudinal section of sperm with complete membrane and regular mitochondria in the control group at day 7 (× 12,000); (D) Semen with oligospermatism and dolichocephalia in the radiation group at day 7 (× 8,000); (E) Semen with high sperm density and sharp axoneme in the TCM treatment group at day 7 (× 12,000).

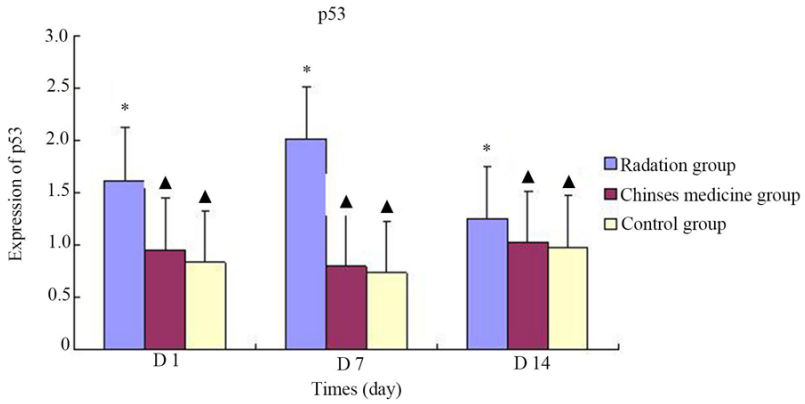

Figure 7. Protein expression of p53 in testis using Western blotting (R: Radiation group; TCM: Chinese Medicine group; C: control group). Expression of p53 on D1, D7, and D14 *Compared with the control group, $p<0.01$; ▲Compared with radiation group, $p<0.01$).

mW/cm^2 HPW, the androgones degenerated, necrotized, and fell off. This was in accord with that of 6 hours following treatment with 10 mW/cm^2 HPW, except that multinucleated giant cells were also observed. At 1 and 7 days, the degeneration aggravated, compared with at 6 hours. After 6 hours of 30/100 mW/cm^2 HPW, androgone degeneration, necrosis, and falling off increased. There was focal necrosis and oligospermatism in the seminiferous tubules. At 3 days after 3 mW/cm^2 HPW, 1-7 days after 10 mW/cm^2 HPW, and 6-7 hours after 30/100 mW/cm^2 HPW, the percentage of teratospermia increased significantly. These previous results suggested that HPM could damage androgones, showing dose- and time-dependent effects.

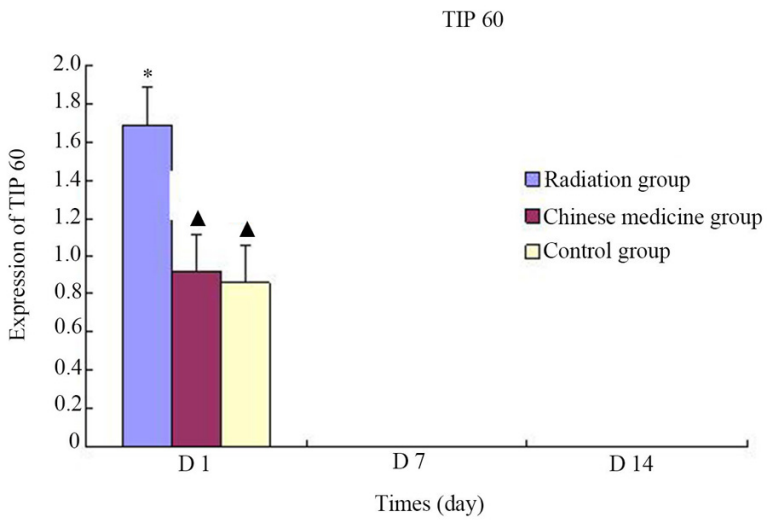

Figure 8. Protein expression of TIP60 in testis using Western blotting (R: Radiation group; TCM: Chinese medicine group; C: control group). Expression of TIP60 on D1. *Compared with the control group, p<0.01; ▲Compared with radiation group, p<0.01).

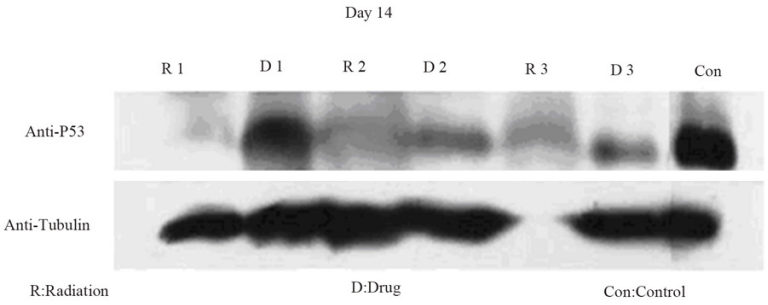

Figure 9. Expression of p53 and tubulin control, radiation, and Traditional Chinese Medicine treatment groups at day 14. Con, control group; R, radiation group; D, Traditional Chinese Medicine treatment group.

Lin et al. [9] used 900 MHz with 250, 150, and 50 μW/cm^2 to treat mice for 24 hours/day for 34.5 days. Following irradiation, they detected the mice capture incubation period (CIP), testis weight ratio, testicular pathological changes, sperm counts, percentage of teratospermia, and testosterone level. They reported that CIP was obviously prolonged (P<0.05), and the testicular pathology changed marginally. Sperm count decreased (P<0.05), the percentage of teratospermia increased (P<0.05), and testosterone levels decreased (P<0.05) in the 150 μW/cm^2 radiation group, compared with the control group. These results indicated that low power microwaves (150 μW/cm^2) induced pathological changes in the testis with decreased CIP and sperm counts, increased teratospermia, and decreased testosterone, influencing mice reproductive abilities.

In the present study, high power microwaves were used to irradiate rats. This led to pathological changes in rats, including increased degeneration of seminiferous tubules, thinning, and falling off limited membrane and seminiferous epithelium. It also led to decreased androgones in different grades and sperm on the luminal surface, androgones falling off, disordered arrangement of seminiferous tubules, sparse interstitial glands, hyaloid degeneration of testicular interstitium, and partial degeneration of sertoli cells. Electron microscopy results showed that the ultrastructure of sperm displayed oligospermatism, dolichocephalia, trochocephalia, congenital acrosome absence, and mitochondrial disorder in the radiation group. Furthermore, apoptosis was increased after irradiation. Results demonstrated that sperm quality, sperm counts, sperm density, and the number of grade A + B sperm were lower in rats exposed to radiation, compared with rats exposed to radiation and treated with TCM extracts. However, the mechanisms remain unclear. Previous studies have demonstrated that the thermal and non-thermal effects of microwave irradiation are the main causes of damage [10-14]. High power microwaves increase tissue temperature and damage physiological function, especially in the testes. Microwave irradiation can lead to ultrastructural changes in the seminiferous epithelium and the epithelia of seminiferous tubules, as well as the perinuclear space. Thus, it contributes to broadening in androgones and sperm, reticulum expansion, mitochondria swelling, and decreased 5-nucleotidase and ATPase activities. Irradiation affects sperm energy metabolism and leads to insufficient support.

This has great effects on sperm physiology and activity levels, indicating that the gonads are highly sensitive to high power radiation [10-14].

A previous study demonstrated that sperm counts and the percentage of sperm in the grade A + B in TCM-treated group was significantly higher than those in other groups. Radiation could increase apoptosis of sperm [8, 15, 16]. In TCM, irradiation has been shown to influence the reproductive system. Long-term radiation may lead to kidney damage, hyposexuality, impotence, premature ejaculation, and infertility [1, 17, 18]. Clinical research has also demonstrated that Traditional Chinese drugs exhibit positive effects on radiation damage [19, 20]. It was hypothesized that the pathogenic effects of microwave irradiation on the body lead to kidney injury, which directly influences the human reproductive system. Results of the current study suggest that the TCM preparation improved sperm quality, increased sperm count, increased sperm density, increased the number of grade A + B sperm, and ameliorated pathological changes in the reproductive system of rats exposed to radiation.

Radiation induces DNA DSB, resulting in mutation, chromosome fragmentation, and even cell death. DNA damage repair is an important reaction in recovering DNA sequence and structure and in sustaining genetic stability. During DNA repair, a series of proteins are activated by post-translational modifications, such as phosphorylation, acetylation, and others [21]. Acetylation is the most common modification in eukaryote cells, with acetyl transferases catalyzing the transfer of an acetyl to a protein. Acetylation has effects on enzymatic activity, protein stability, DNA binding ability, and interaction between proteins. Histone acetylation is a major method of epigenetic regulation. It coordinates with other histone and DNA modifications to regulate the histone code. The histone code can be identified by transcription factors to regulate transcription. The MYST family of acetyltransferases includes lysine acetyltransferase 6A, TIP60, and others [22]. It has been demonstrated that the stable TIP60 complex can modify histones, assembling within the plasmosome *in vitro [*23, 24]. Additionally, TIP60 can acetylate transcription factors, including androgen receptors, upstream binding transcription factors, C-myc, and ATM serine/threonine kinase, enhancing stability and transcriptional activity. Moreover, p53 can be acetylated at a specific lysine by acetyltransferases [25]. Thus, p53 acetylation plays an important role in p53-dependent transcriptional activation, cell apoptosis, tumor pathogenesis, and DNA damage [26, 27]. TIP60 has been shown to interact with p53 *in vivo* and *in vitro* [28-30]. It has been reported that, upon DNA damage, TIP60 specifically acetylates lysine 120 on the DNA binding domain of p53. Thus, when there is DNA damage, TIP60 can influence the choice of promoter, regulate the switch from cell cycle arrest to apoptosis, promote p53, and mediate apoptosis, indicating that TIP60-dependent acetylation on p53 lysine 120 is crucial for cell apoptosis and DNA damage [31].

In the present study, downstream signaling molecules of TIP60 were investigated by deficiencies of TIP60. This was to explain the biochemical pathways associated with microwave irradiation damage and repair. There was TIP60 expression in the early period (1 day) following radiation, but not in the middle (7 days) and late (14 days) period. However, p53 was expressed in the early, middle, and late period, with higher expression in the TCM treatment group, compared with the radiation group. There were no differences in tubulin expression between the TCM treatment group and radiation groups. It was hypothesized that microwave irradiation caused DNA damage and induced the upregulation of TIP60 acetyltransferase. Increasing p53 acetylation, TIP60 participated in the initial stages of DNA repair. Less expression of TIP60 without acetylation activity resulted in the loss of DNA DSB repair ability and increased apoptosis. Current results suggest that TIP60, a co-activator of p53, synergistically participates in DNA repair. It plays a critical role in DNA damage response and DNA repair. TCM treatment, in the current study, increased p53 expression. This may promote DNA repair, sperm activity, and sperm density. However, further investigation is necessary.

In conclusion, radiation may damage DNA and improve the HAT activity of TIP60. Regulation of DNA repair or apoptosis may be enhanced by increasing acetylase levels of p53. Moreover, TCM may significantly improve p53 signaling pathways in this process. Thus, it promotes DNA repair and improves sperm activity and density.

Address correspondence to: Dr. Ti-Ye Sun, Department of Gerontology, General Hospital of The Air Force, 30 Fucheng Road, Haidian, Beijing 100142, P. R. China. E-mail: suntite_09@163.com

References

[1] Hu HX, Fang H, Luo SB, Dong J and Wei LZ. Microwave radiation of radar operators ultrastructure of sperm head and tail. zhonghuanankexuezazhi 2010; 24: 33-35.

[2] Sapountzi V, Logan IR, Robson CN. Cellular functions of TIP60. Int J Biochem Cell Biol 2006; 38: 1496-1509.

[3] Sapountzi V, Logan IR, Nelson G, Cook S, Robson CN. Phosphorylation of Tat-interactive protein 60 kDa by protein kinase C epsilon is important for its subcellular localization. Int J Biochem Cell Biol 2008; 40: 236-244.

[4] Xu S, Panikker P, Iqbal S, Elefant F. Priyalakshmi panikker, sahira iqbal, felice elefant. TIP60 HAT action mediates environmental enrichment induced cognitive restoration. PLoS One 2016; 11: e0159623.

[5] Ikura T, Ogryzko VV, Grigoriev M, Groisman R, Wang J, Horikoshi M, Scully R, Qin J, Nakatani Y. Involvement of the TIP60 histone acetylase complex in DNA repair and apoptosis. Cell 2000; 102: 463-473.

[6] Bird AW, Yu DY, Pray-Grant MG, Qiu Q, Harmon KE, Megee PC, Grant PA, Smith MM, Christman MF. Acetylation of histone H4 by Esa1 is required for DNA double-strand break repair. Nature 2002; 419: 411-415.

[7] World Health Organization laboratory manual for the examination and processing of human semen (third edition), 1992; 5-62.

[8] Wang SM, Peng RY, Gao YB, Ma jj, Chen HY and Zhou HM. Testicular injury in rats caused by high power microwave radiation of pathology research. zhonghuanankexuezazhi 2006; 12: 486-489.

[9] Lin MD, Chen Y, Chen H, Lin MD, Wang XJ. Different intensity of low power microwave radiation effects on reproductive system of male mice. aibianqibiantubiantubian 2007; 19: 494-496.

[10] Li R, Liu LC, Wang FJ and Wang W. Effects of morinda officinalis how on testicular injury induced by microwave radiation in adult male rats. Jiepouxuezazhi 2014; 37: 22-24.

[11] Buckus R, Strukcinskiene B, Raistenskis J, Stukas R. Modeiling and assessment of the electric field strength caused by mobile phone to the human head. Vojnosanit Pregl 2016; 73: 538-543.

[12] Geng TQ, Luo Q, Wang AJ, Jun Y, Xiao YC and Jing JL. Effects of lyceum barbarum polysaccharide on testicular cell apoptosis induced by low dose Ionizing radiation in male rats. Acta Nutrimneta Sinica 2014; 36: 608-611.

[13] Yuan M, Lin YY, Guo QY, Gao P, Miao X, Lang HY, Zhang JP, Yuan YK, Liu JY and Zeng LH. Effects of 1840 MHz electromagnetic radiation on sex hormones and antioxidant damage in male SD rats. Xiandaishengwuyixuejinzhan 2017; 28: 5406-5411.

[14] Li R, Yang WQ and Wang W. Effects of water extract and alcohol extract from Morinda officinalis how on injury of hypothalamus pituitary gonad axis in rats induced by cell phone radiation. Zhongguolinchuangyaolixuezazhi 2016; 32: 1881-1885.

[15] Gao XF, Wang SM, Peng RY and Gao YB. Effects of high power microwave radiation on blood testis barrier in rats. Zhonghuanankexuezazhi 2008; 14: 579-582.

[16] Wang CY. Effects of high intensity microwave radiation on reproductive system in male rats. Jilinyiyaoxueyuanxuebao 2015; 36: 338-340.

[17] Wang SM, Peng RY, Gao YB, Chang GM, Dong Q, Zhang J, Su ZT. Effect of Ando Lin on epididymal sperm parameters in rats exposed to microwave radiation. Zhongguoshengyujiankangzazhi 2012; 23: 191-194.

[18] Xu SQ, Hu HX, Luo SB, Wei LZ, Jing D, Ding HH, Gao YJ, Song XL, Yu X, Li JC. Effects of radar microwave radiation on sex hormones and semen quality of workers. Jiefangjunyiyaozazhi 2013; 25: 41-43.

[19] Bi HZ. The electromagnetic radiation damage hot pathogenesis theory. Zhongguozhongyijichuyixuezazhi 2001; 17: 576-578.

[20] Hu HX, Luo SB, Sun J, Wei LZ, Dong J, Liu HY, Xu SQ, Zhang D. Effects of yiqi yangyin shengjing recipe on reproduction of male rats under microwave irradiation. Beijingzhongyiyaodaxuexuebao 2013; 36: 250-253.

[21] Haber JE. Partners and pathways repairing a double-strand break. Trends Genet 2000; 16: 259-264.

[22] Thomas T, Loveland KL, Voss AK. The genes coding for the MYST family histone acetyltransferases, TIP60 and Mof, are expressed at high levels during sperm development. Gene Expr Patterns 2007; 7: 657-665.

[23] Fan R, Liu XD, Wang Y, Xu QZ, Zhou PK. Effect of TIP60 over expression on cell DNA radiation damage repair and cell cycle. Fushefanghu 2012; 32: 83-86.

[24] Fan R, Zhang SM, Liu XD, Wang Y, Xu QZ, Zhpu PK. Effects of TIP60 gene silencing on repair and radiosensitivity of DNA double strand breaks in cells. Zhonghuafangsheyixueyufanghuzazhi 2011; 31: 511-514.

[25] Cui H, Li X, Han C, Wang QE, Wang H, Ding HF, Zhang J, Yan C. The stress-responsive gene ATF3 mediates dichotomous UV responses by

regulating the TIP60 and p53 proteins. J Biol Chem 2016; 291: 10847-10857.
[26] Wang Q, Goldstein M. Small RNAs recruit chromatin-modifying enzymes MMSET and TIP60 to reconfigure damaged DNA upon double-strand break and facilitate repair. Cancer Res 2016; 76: 1904-15.
[27] Sun W, Ma XM, Ding JB, Guo H, Zhu YH, Xu LJ and Bai JP. Expression and relationship of PDCD5, MDM2, TIP60 and p53 in esophageal squamous cell cancer. Basic & Clinical Medicine 2011; 31: 847-852.
[28] Fan R, Zhang SM, Liu XD, Wang Y, Xu QZ and Zhou PK. Deficiency of DNA double-strand break repair and enhanced radiosensitivity in TIP60 silenced cells. Chinese Journal of Radiological Medicine and Protection 2011; 31: 511-514.
[29] Chailleux C, Tyteca S, Papin C, Boudsocq F, Pufet N, Courilleau C, Grigoriev M, Canitrot Y and Trouche D. Physical interaction between the histone acetyl transferase TIP60 and the DNA doublestrand breaks sensor MRN complex. Biochen J 2010; 426: 365-371.
[30] Sakuraba K, Yokomizo K, Shirahata A, Goto T, Saito M, Ishibashi K, Kigawa G, Nemoto H and Hibi K. TIP60 as a potential marker for the malignancy of gastric cancer. Anticancer Res 2011; 31: 77-79.
[31] Sykes SM, Mellert HS, Holbert MA, Li K, Marmorstein R, Lane WS and McMahon SB. Acetylation of the p53 DNA binding domain regulation apoptosis induction. MoL Cell 2006; 24: 841-851.